A multicomponent assembly approach for the design of deep desulfurization heterogeneous catalysts

Yanqi Xu,[a] Weimin Xuan,[a] Mengmeng Zhang,[a] Haralampos N. Miras*[b] and Yu-Fei Song[a]*

Deep desulfurization process is a challenging task and global efforts are focused on the development of new approaches for the reduction of sulfur-containing compounds in fuel oils. In this work, we have proposed a new design strategy for the development of deep desulfurization heterogeneous catalysts. Based on the adopted design strategy, a novel composite material of polyoxometalate (POM)-based ionic liquid-grafted layered double hydroxides (LDHs) was synthesized by an exfoliation/grafting/assembly process. The structural properties of the as-prepared catalyst were characterized using FT-IR, XRD, TG, NMR, XPS, BET, SEM and HRTEM. The heterogeneous catalyst exhibited high activity in deep desulfurization of DBT (dibenzothiophene) 4,6-DMDBT (4,6-dimethyldibenzothiophene) and BT (benzothiophene) at 70 °C in 25, 30 and 40 minutes, respectively. The catalyst can be easily recovered and reused for at least ten times without obvious decrease of its catalytic activity. Such excellent sulfur removal ability as well as the cost efficiency of the novel heterogeneous catalyst can be attributed to the rational design, where the spatial proximity of the substrate and the active sites, the immobilization of ionic liquid onto the LDHs *via* covalent bonding and the recyclability of the catalyst are carefully considered.

Introduction

Based on the severe environmental impact of sulfur-containing compounds in fuel oils, rendered the development of efficient deep desulfurization processes one of the global urgent tasks.[1] Currently, the hydro-desulfurization (HDS) process is widely used in industry to remove sulfur-containing compounds from oils.[2] Specifically, HDS process is an efficient method for removing thiols, sulfides and disulfides from fuel oils.[3-7] However, the removal of DBT, 4,6-DMDBT and BT *etc*. *via* HDS processes is quite challenging. Moreover, the harsh conditions of the HDS process such as high pressure and high temperature restrict its wide application for deep desulfurization. In contrast to the HDS, oxidative desulfurization (ODS) processes require relatively mild reaction conditions.[8-11] As one of the most promising ODS processes, extractive and catalytic oxidative desulfurization (ECODS) process, where ionic liquids (ILs) are used as extractants and H_2O_2 is used as oxidant, has been extensively investigated.[12-14] The combination of extractive and oxidative desulfurization, rendered ECODS as a highly efficient method for the production of clean fuels.[15-17]

The last decades, utilization of ILs as extractants in ECODS processes have been intensively studied due to their unique physicochemical properties such as negligible vapor pressure, tunable solubility or extracting capability for inorganic or organic compounds, high thermal/chemical stability, non-flammability, non-toxicity and so on.[2, 18] ILs is a highly promising family of compounds with extracting properties for the efficient manufacturing of clean fuel oils in the near future. However, the high cost and recycling challenges restrict the extensive utilization of ILs' in industrial scale desulfurization applications. These issues are the main challenges the scientific groups are currently facing.

On the basis of structural characterization of the heterogeneous desulfurization catalysts reported so far and in line with the green chemistry principles, rational design of a heterogeneous catalyst of ECODS should meet the following requirements: 1) the substrate candidates (DBT, BT and 4,6-DMDBT) should be able to get access to the active catalytic sites easily. To improve the phase transfer ability for a heterogeneous catalyst, ionic liquids are frequently used to provide the suitable environment to enhance phase transfer as well as the spatial proximity between substrates and the catalytic active component;[19,20] 2) the supports should not only exhibit strong interactions with the active components, but also provide the necessary structural integrity which will prevent the leaching of the active components;[21, 22] 3) most importantly, the catalysts should retain their reactivity and structural stability during recycling process.[23, 24]

Herein, we report the design and preparation of an heterogeneous catalyst, Mg_3Al-IL-EuW_{10}, which was prepared by intercalating $Na_9(EuW_{10}O_{36})\cdot 32H_2O$ (Na-EuW_{10}) clusters into the ionic liquids (ILs) modified layered double hydroxides (LDHs). The extractive and oxidative desulfurization experiments indicate that almost 100 % sulfur removal of DBT, 4,6-DMDBT and BT can be achieved using Mg_3Al-IL-EuW_{10} as catalyst and H_2O_2 as oxidant at 70 °C in 25, 30 and 40 min, respectively.

Experimental

2.1 Materials

Hexamethylenetetramine (HMT, 99 %), $Mg(NO_3)_2\cdot 6H_2O$ (99 %), $Al(NO_3)_3\cdot 9H_2O$ (99 %), formamide (99 %), $Na_2WO_4\cdot 2H_2O$ (99 %), acetic acid (99 %), $EuCl_3\cdot 6H_2O$ (99 %), dibenzothiophene (DBT), 4,6-dimethyldibenzothiophene (4,6-DMDBT), benzothiophene (BT), hydrogen peroxide (30 wt.% H_2O_2), *n*-octane (99 %), and all used solvents (analytical grade) were obtained from Alfa Aesar and were used directly without any further purification. N-[3-(triethoxysilyl)propyl]-4,5-dihydroimidazolium was purchased from Sigma-Aldrich and used directly as received.

2.2 Characterization

Fourier transform infrared (FT-IR) spectra were recorded on a Bruker Vector 22 infrared spectrometer by using KBr pellet method. The powder X-ray diffraction (XRD) analysis was carried out on a Bruker D8 diffractometer with high-intensity Cu-Ka radiation (λ = 0.154 nm). Thermogravimetric (TG) analysis was carried out using a STA-449C Jupiter (HCT-2 Corporation, China) at a heating rate of 10 ^{o}C min^{-1} from 25 to 1000 ^{o}C under N_2 atmosphere (20 mL/min). ^{1}H and ^{13}C NMR spectra were recorded on a Bruker AV400 NMR spectrometer at 400 MHz. The solid-state NMR experiments were carried out on a Bruker Avance 300M solid-state spectrometer equipped with a commercial 5 mm MAS NMR probe. N_2 adsorption-desorption isotherms were measured using Quantachrome Autosorb-1 system at liquid nitrogen temperature. BET measurements were performed at 77 K on a Quantachrome Autosorb-1C analyzer. Scanning electron microscopy (SEM) images were obtained using a Zeiss Supra 55 SEM. High resolution transmission electron microscopy (HRTEM) images and energy dispersive X-ray (EDX) analytical data were collected on a JEOL JEM-2010 electron microscope operating at 200 kV. Inductively coupled plasma-atomic emission spectroscopy (ICP-AES) analysis was performed on a Shimadzu ICPS-7500 instrument. X-ray photoelectron spectroscopy (XPS) measurements were performed using a monochromatized Al K exciting X-radiation (PHI Quantera SXM). The contents of DBT, 4,6-DMDBT and BT were analyzed on an Agilent 7820A GC system using a 30 m 5 % phenylmethyl silicone capillary column with an ID of 0.32 mm and 0.25 mm coating (HP-5).

2.3 Synthesis of Mg_3Al-IL-EuW_{10}

Chemicals: The 1-octyl-3-(3-triethoxy-silylpropyl)-4,5-dihydroimidazolium hexafluoro-phosphate (IL-PF_6), $Na_9(EuW_{10}O_{36})\cdot 32H_2O$ (Na-EuW_{10}) and Mg_3Al-NO_3 were synthesized according to the method reported previously.[25-27] The FT-IR spectrum and XRD pattern of Mg_3Al-NO_3 as well as the FT-IR spectrum, ^{1}H CP/MAS NMR and ^{13}C CP/MAS NMR spectra of IL-PF_6 are shown in supporting information.

Synthesis of Mg_3Al-IL-EuW_{10}: The Na-EuW_{10} was intercalated into Mg_3Al-NO_3 *via* an exfoliation/assembly process under N_2 atmosphere.[28, 29]

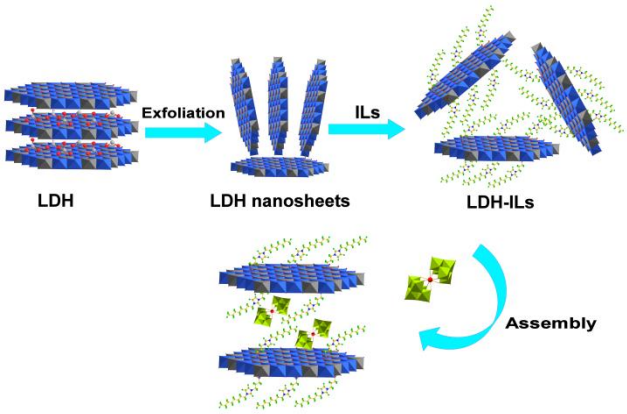

Scheme 1. The synthetic procedure for the preparation of the designed heterogeneous catalyst of Mg_3Al-IL-EuW_{10}.

Synthesis of Mg_3Al-IL-EuW_{10}: Mg_3Al-NO_3 (1.0 g) was dispersed in 1000 mL of formamide solution and then the reaction mixture was kept stirring for 48 h under N_2 atmosphere at 25 ^{o}C. Then, IL-PF_6 (8.8 mmol) was added into the above suspension and the reaction mixture was stirred for 24 h. Finally, Na-EuW_{10} (3.5 g) was added to the above solution and a white precipitate was formed after 12 h. Then, the precipitate (≈ 2.0 g) was filtered, washed with ethanol (3 × 50 mL) and water (2 × 50 mL) and dried under vacuum overnight (Scheme 1).

2.4 Extractive and oxidative catalytic desulfurization procedure

In a typical experiment, model oils were prepared by dissolving DBT or 4,6-DMDBT or BT in *n*-octane with total S-content of 1000 ppm. A mixture including catalyst (0.02 mol EuW_{10}), 0.08 mL H_2O_2 and 5 mL model oil containing DBT (S = 1000 ppm) in a flask was stirred vigorously for 25 minutes at 70 ^{o}C. 0.1 μL of the reaction mixture was injected to the gas chromatography to monitor the progress of the desulfurization.

3. Results and discussion

3.1 Structure analysis

The FT-IR spectrum of Na-EuW_{10} stretching bands located at 948, 850, 791 and 697 cm^{-1}, which can be assigned to the W-O_t, W-O_c-W and W-O_e-W vibrations, respectively, where O_t denotes the terminal oxygens, O_c the corner shared oxygens and O_e the edge sharing oxygen atoms between two neighbouring octahedra (Fig. 1A).[30] The characteristic vibration peaks are located at 947, 834, 779 and 656 cm^{-1} in the corresponding FT-IR spectrum of Mg_3Al-EuW_{10} (Fig. 1A). In the case of MgAl-IL-EuW_{10}, the corresponding FT-IR spectrum exhibits the C-H stretching vibrations at 2930 and 2856 cm^{-1} due to the alkyl chain -CH_2- and -CH_3 whilst the C=N stretching vibration located at 1658 cm^{-1} due to the imidazole component of the ILs component (Fig. S1), respectively. In addition, the W-O stretching bands appear at 942, 844, 775, and 691 cm^{-1}, respectively. Comparing with the LDH based starting material, Mg_3Al-NO_3 (Fig. S1), the absence of the vibration bands at 1383 cm^{-1} for NO_3^- and the presence of characteristic bands of EuW_{10} in the FT-IR spectrum of Mg_3Al-IL-EuW_{10} indicate the successful intercalation of the EuW_{10}

cluster. In addition, the absorption band at 447 cm^{-1} can be ascribed to O-M-O (M = Mg and Al) vibrations in the brucite-like layers of the LDHs (Fig. 1A).[31-34]

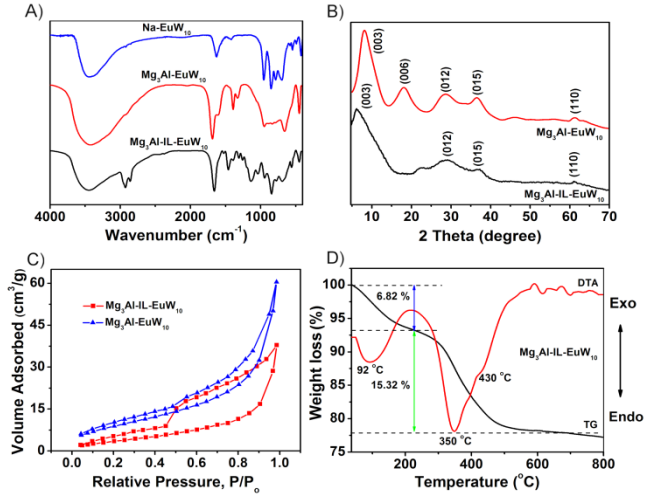

Fig. 1. A) FT-IR spectra of Na-EuW_{10}, Mg_3Al-EuW_{10} and Mg_3Al-IL-EuW_{10}; B) XRD patterns of Mg_3Al-EuW_{10} and Mg_3Al-IL-EuW_{10}; C) The N_2 adsorption-desorption isotherms of Mg_3Al-EuW_{10} and Mg_3Al-IL-EuW_{10}; D) TG-DTA characterization of Mg_3Al-IL-EuW_{10}.

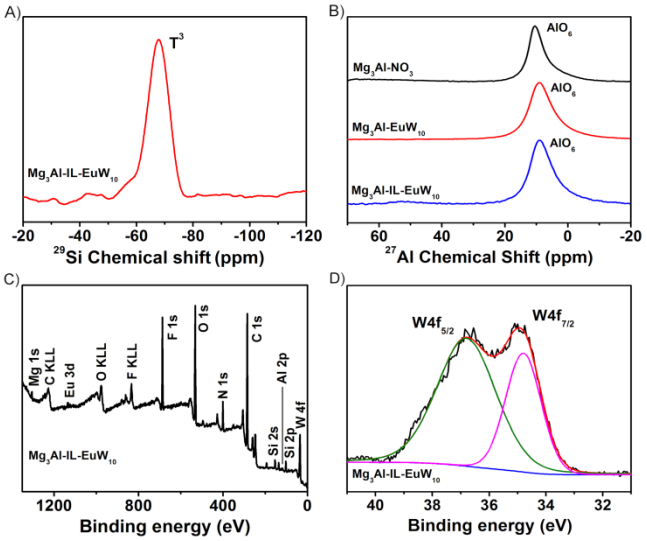

Fig. 2. A) The ^{29}Si CP/MAS NMR spectrum of Mg_3Al-IL-EuW_{10}; B) The ^{27}Al CP/MAS NMR spectra of Mg_3Al-NO_3, Mg_3Al-EuW_{10} and Mg_3Al-IL-EuW_{10}; XPS spectra of the C) Mg_3Al-IL-EuW_{10} material; D) W core levels of the Mg_3Al-IL-EuW_{10}.

Comparison of the Mg_3Al-EuW_{10} XRD patterns with the parent LDH, Mg_3Al-NO_3 (Fig. S2), revealed that the basal (003) and (006) composite's reflections shift to lower 2ϑ angles at 7.97° and 17.83°, respectively. The gallery height found to be 0.78 nm and was calculated by subtracting the thickness of the host layer (0.48 nm), indicating that the EuW_{10} anions intercalated with their C_4 axis aligned parallel to the Mg_3Al-LDHs layers.[35] In the case of Mg_3Al-IL-EuW_{10}, the basal (003) reflection shifts to much lower 2ϑ angle (5.874°) and the gallery height in this case is 1.02 nm. Thus, the orientation of the EuW_{10} anions' C_4 axis intersects the LDH layers at an angle of ca. 45°. Additionally, the XRD pattern of Mg_3Al-IL-CO_3 was used to investigate the ILs effect on the stacking of LDHs layers (Fig. S2). The basal reflections of Mg_3Al-IL-CO_3 appeared to be broader without any obvious shifting, highlighting the inefficiency of ILs on its own to induce structural stability by acting as robust pillars between the LDHs layers.

The N_2 adsorption-desorption isotherm of Mg_3Al-IL-EuW_{10} (Fig. 1C) displays the typical IV isotherm pattern with capillary condensation taking place in mesopores, and H4-type hysteresis loop associated with narrow slit-like pores, indicative of the mesoporous feature of the catalyst.[36] As can be seen from Table S1, the surface area and pore size measured for Mg_3Al-EuW_{10} and Mg_3Al-IL-EuW_{10} are 33.61 m^2g^{-1} and 4.20 nm, 41.82 m^2g^{-1} and 5.78 nm, respectively.

Thermogravimetric (TG) curve of Mg_3Al-IL-EuW_{10} (Fig. 1D) exhibits two mainly consecutive weight-loss steps from 25 to 685 °C. The first weight loss of 6.82 wt.% taking place between 25 and 225 °C can be assigned to the loss of surface-adsorbed and interlayer water molecules. The second weight loss of 15.32 wt.% observed in the range of 225-685 °C can be attributed to the collapse of the layered structure and decomposition of the anchored ILs on the LDHs. Additionally, DTA curve shows two endothermic peaks centred at 350 and 430 °C, corresponding to the destruction of laminate structure and the loss of ILs from the host layers, respectively.[28, 29, 37] Based on the elemental and ICP analysis [Mg = 12.47 wt.%, Al = 4.14 wt.%, W = 36.98 wt.%, C = 5.57 wt.%, H = 2.90 wt.%, N = 0.94 wt.%], the composition of Mg_3Al-IL-EuW_{10} can be expressed as $[Mg_{0.77}Al_{0.23}(OH)_{1.85}(C_{14}H_{28}N_2O_3Si)_{0.05}][EuW_{10}O_{36}]_{0.03}[PF_6]_{0.01}\cdot 0.59H_2O$. As a result, the loading of EuW_{10} and ILs components in the Mg_3Al-IL-EuW_{10} composite are 45.28 wt.% and 10.99 wt.%, respectively.

The solid state ^{29}Si CP/MAS NMR (Fig. 2A) was used to estimate the local environments of Si^{4+} in the Mg_3Al-IL-EuW_{10}. Mg_3Al-IL-EuW_{10} displays one set of resonance signal at -68 ppm, which can be assigned to T^3 organo-silica species of ILs that are covalently grafted onto the LDHs layers *via* formation of oxane bonds M-O-Si (M = Mg and Al in LDHs layers).[38] The solid-state ^{27}Al CP/MAS NMR analysis (Fig. 2B) has been carried out to examine the local environment of Al^{3+} in the corresponding Mg_3Al-NO_3, Mg_3Al-EuW_{10} and Mg_3Al-IL-EuW_{10}. It is known that the ^{27}Al resonance line positions are greatly depend upon the coordination number and are expected to appear within a broad range of ppm values; sites which adopt octahedral geometry (AlO_6) cover the range between -5 to 15 ppm while sites with tetrahedral geometry (AlO_4) span the range 60 - 90 ppm.[39] The Mg_3Al-NO_3, Mg_3Al-EuW_{10} and Mg_3Al-IL-EuW_{10} revealed only one peak centred at δ_{Al} = 10.50, 9.47 and 9.07 ppm, respectively, indicating that the Al^{3+} adopts octahedral geometry. The chemical shift towards high field for Al^{3+} in Mg_3Al-IL-EuW_{10} can be attributed to the interactions between the host layers and intercalated EuW_{10} clusters.

XPS measurement has been employed in order to characterize the surface chemical composition and oxidation state of the catalyst. Fig. 2C, presents peaks attributed to Mg, Al, C, O, N, Si, Eu and W. The binding energies of $W4f_{7/2}$ and

W4f$_{5/2}$ found to be 35.1 and 36.7 eV, respectively, suggesting the presence of W(VI) in Mg_3Al-IL-EuW_{10} (Fig. 2D).

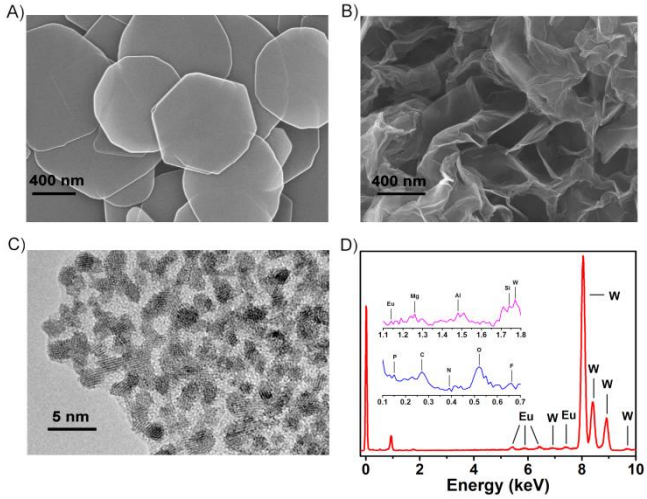

Fig. 3. SEM images of A) Mg_3Al-NO_3 and B) Mg_3Al-IL-EuW_{10}; C) HRTEM images of Mg_3Al-IL-EuW_{10}; D) EDX of Mg_3Al-IL-EuW_{10}.

The SEM image of Mg_3Al-NO_3 revealed the porous stacking of sheet-like material with particle sizes of ca. 1 μm, whilst the Mg_3Al-IL-EuW_{10} composite maintains the laminated structure with size of approximately of 500 nm (Fig. S4). In contrast to the flat hexagonal feature of Mg_3Al-NO_3, the curly morphology of Mg_3Al-IL-EuW_{10} can be attributed to the increased percentage of non-bonded atoms at the edges after the exfoliation/grafting/assembly process.[40] HRTEM image of Mg_3Al-IL-EuW_{10} (Fig. 3C) confirms that the EuW_{10} clusters are highly dispersed into the ILs modified LDHs without evidence of agglomeration. The HRTEM-EDX of Mg_3Al-IL-EuW_{10} provides further evidence to confirm the successful modification with IL-PF_6 and intercalation of EuW_{10} (Fig. 3D).

3.2 Catalytic performance of desulfurization

Before investigating the efficiency of our composite material using an actual model oil system it was necessary to determine the optimum operational parameters for the catalytic process through a series of tests and control experiments. As shown in Fig. 4A, the oxidation of DBT has been investigated at different temperatures in order to evaluate initially, the effect of temperature on the catalytic activity of Mg_3Al-IL-EuW_{10}. The result demonstrates that 55 and 73 % sulfur removal can be obtained at 30 and 40 ^oC, respectively in 140 min. When the temperature increases to 50, 60 and 70 ^oC, almost 100 % removal of DBT can be achieved in 135, 40 and 25 min, respectively. Thus, 70 ^oC has been chosen as the optimized temperature and used for the subsequent experiments.

In order to gauge the influence of H_2O_2/DBT molar ratio on the sulfur removal under the experimental conditions (T = 70 ^oC, DBT/EuW_{10} = 8:1, S = 1000 ppm), a series of experiments have been performed. As shown in Fig. 4B, when the H_2O_2/DBT molar ratio increases from 3:1 to 4:1, the time for sulfur removal over 99 % is shortened from 80 to 70 min. A further increase of H_2O_2/DBT molar ratio to 5:1 results in almost 100 % sulfur removal of DBT in 25 min. Thus we concluded that the 5:1 H_2O_2/DBT is the optimum molar ratio for the subsequent catalytic studies. Finally, decrease of the DBT/EuW_{10} molar ratio from 16:1, 8:1 to 4:1 in the presence of 0.08 mL H_2O_2, we observed a decrease of the time required to achieve deep desulfurization from 35 to 25 and 15 min, respectively (Fig. 5A). Thus, we used DBT/EuW_{10} = 8:1 molar ratio at 70 ^oC for our subsequent experiments.

In an effort to determine the catalytic efficiency of the Mg_3Al-IL-EuW_{10} composite material, we measured the required desulfurization time for various concentrations of DBT (Fig. 5B). When the S content is as low as 50 ppm (S = 50 ppm), deep desulfurization can be achieved in 8 min; When the volume of model oil reaches 1000 mL (S = 1000 ppm), 100 % sulfur removal can be obtained in 55 min.

It is well established that the thiophene sulfides account for more than 80 % of the total sulfur content in diesel fuel, whilst DBT, BT and 4,6-DMDBT account for 70 % of it. Therefore, the removal of the thiophene sulfides is a top priority. To demonstrate the catalytic activity of Mg_3Al-IL-EuW_{10}, sulfur removal of 4,6-DMDBT and BT have been carried out under the same conditions.[41] The experimental data revealed that almost 100 % sulfur removal could be achieved within 30 and 40 min for 4,6-DMDBT and BT, respectively, under the same experimental conditions as above (Fig. 5B). As such, the sulfur removal capability decreases in the order of DBT > 4,6-DMDBT > BT, owing to the different electron densities on the sulfur atom of DBT (5.75), 4,6-DMDBT (5.76) and BT (5.73), respectively.[42] As the electron density on the sulfur atom of BT is the lowest one among all substrates, it took longer to be removed from the oil mixture. In the case of 4,6-DMDBT and DBT, the two methyl groups of 4,6-DMDBT induce considerable steric hindrance which affects the desulfurization process, and this is reflected on the observed rate for sulfur removal.

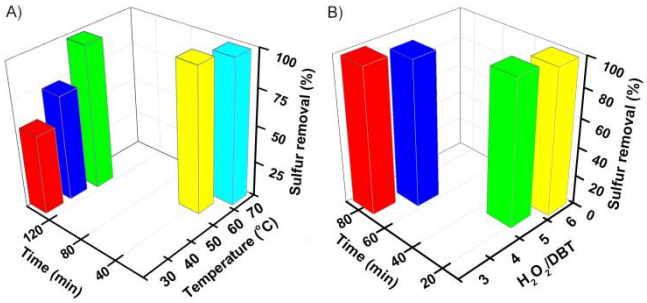

Fig. 4. A) Effect of temperature and B) Effect of H2O2/DBT molar ratio on sulfur removal of DBT. Reaction conditions: A) H2O2/DBT/EuW10 = 40:8:1 (H2O2 = 0.08 mL, model oil = 5 mL, S = 1000 ppm); B) DBT/EuW10 = 8:1 (T = 70 oC, model oil = 5 mL, S = 1000 ppm).

The coexistence of other components in the oily phase, such as aromatic hydrocarbon, olefins and so on, may reduce the efficiency of desulfurization as they may be involved in side reactions that might take place under the oxidizing environment. In this regard, paraxylene, 1-octene and cyclohexene were chosen as representative substances and added to the model oil in order to explore the effect of these additives on the desulfurization process. Fig. 5C, revealed that the presence of paraxylene and 1-octene has no obvious effect on the desulfurization efficiency. In the case of cyclohexene,

we observed a decrease of the sulfur removal from 99.9 % to 90 %, which indicates that it would be preferable removing the cyclic olefin before initiating the desulfurization process.

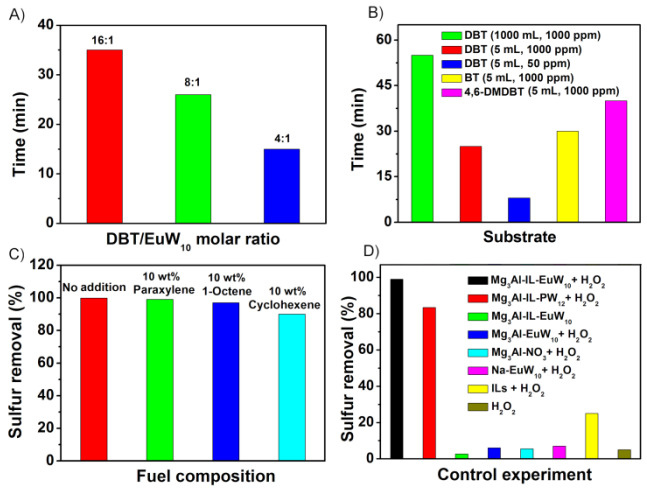

Fig. 5. A) Effect of DBT/EuW_{10} molar ratio on sulfur removal of DBT; B) Effect of Mg_3Al-IL-EuW_{10} on sulfur removal of DBT, BT and 4,6-DMDBT; C) Effect of fuel composition on sulfur removal of DBT. D) Effect of different catalysts on sulfur removal of DBT.

Additional, control experiments were carried out using different desulfurization systems under the same experimental conditions (Fig. 5D). It was observed that less than 5 % of desulfurization can be obtained using only H_2O_2, whereas ILs in the presence of H_2O_2 results in 25 % sulfur removal of DBT. Similar poor performance was measured also in the case of Mg_3Al-NO_3/H_2O_2, Na-EuW_{10}/H_2O_2 or Mg_3Al-EuW_{10}/H_2O_2 catalytic system, where less than 10 % sulfur removal could be achieved. In an additional control experiment, we intercalated the commercially available $Na_3[PW_{12}O_{40}]$ cluster into the IL-modified LDHs giving the Mg_3Al-IL-PW_{12} composite and tested its efficiency in deep desulfurization processes. The Mg_3Al-IL-PW_{12}/H_2O_2 system demonstrated inferior performance, and revealed an 83.38 % sulfur removal of DBT in 25 min at 70 °C. In contrast, utilization of the Mg_3Al-IL-EuW_{10} composite we achieved almost 100 % of the sulfur removal of DBT in the presence of H_2O_2. It is worth noting that pure Mg_3Al-IL-EuW_{10} in the absence of H_2O_2 demonstrated less than 5 % of sulfur removal.

It is meaningful at this point to compare the catalytic oxidative desulfurization of DBT by previously reported heterogeneous catalysts (Table 1). A few supported catalysts containing molybdenum, V_2O_5 or WO_x were used for catalytic oxidative desulfurization of DBT and the best desulfurization result was 98.1 % of sulfur removal (Table 1, entries 1-4). Utilization of $H_3PW_{12}O_{40}$ or $H_4SiMo_{12}O_{40}$ containing catalysts (Table 1, entries 5-13), demonstrated efficient deep desulfurization only after prolonged reaction times. In the case of the sandwich-type POM catalyst (Table 1, entry 14), 100 % sulfur removal can be achieved at 70 °C, after 2 h but only using mixture of considerably lower S-content (500 ppm). For the graphene-analogous boron nitride supported catalysts containing tungsten-based ionic liquids or tungsten oxide nanoparticles (Table 1, entry 15-16), deep desulfurization can be achieved in 80 min for sulfur load of S = 500 ppm. In the case of non-carrier catalyst, the hexagonal boron nitride nanosheets (h-BNNs) (Table 1, entry 17) shows high efficiency for deep desulfurization under extreme operating conditions. Compared with other systems, Mg_3Al-IL-EuW_{10} shows high efficiency for deep desulfurization at 70 °C in 25 min at S = 1000 ppm, which shows great potential for further application.

3.3 Kinetic studies

In order to have a better understanding of the desulfurization kinetics of the catalytic process, ECODS of DBT has been performed using the previously determined optimized reaction parameters, H_2O_2/DBT/EuW_{10} = 40:8:1 at 70 °C, and followed the reaction as a function of the time. The results are summarized in Fig. 6, where the catalytic reaction follows a pseudo-first-order kinetics with R^2 = 0.9931. The percentage of sulfur removal and $\ln(C_t/C_0)$ are plotted against reaction time, where C_0 and C_t are the DBT concentration at t = 0 min and t min, respectively, while k is the rate constant

Table 1. Comparison of catalytic oxidative desulfurization of DBT by different heterogeneous catalysts.

Entry	Catalyst	Extractant	T/°C	t/min	S/ppm	S removal/%	Ref.
1	Mo/γ-Al_2O_3	CH_3CN	60	75	320	98	43
2	Mo/MMS	DMF	103	62	500	98.1	44
3	V_2O_5/TiO_2	-	60	120	600	82	45
4	WO_x/TiO_2	-	60	360	1472	85	46
5	$[Bmim]_3PW_{12}O_{40}/SiO_2$	DMF	80	180	445	98.2	47
6	$H_3PW_{12}O_{40}/TiO_2$	CH_3CN	60	120	500	95.2	48
7	$H_3PW_{12}O_{40}$–TiO_2–SiO_2	CH_3CN	70	120	1000	100	49
8	$H_3PW_{12}O_{40}$-HMS-DS	CH_3CN	60	120	500	99	50
9	$H_3PW_{12}O_{40}$-TUD-1	CH_3CN	60	180	500	98.1	51
10	$H_3PW_{12}O_{40}/SiO_2$	CH_3CN	60	60	500	98.8	52
11	$H_3PW_{12}O_{40}$–PDMAEMA–SiO_2	-	60	180	500	100	53
12	$[C_{16}mim]_3PW_{12}O_{40}$/MCM-41	-	60	30	500	99.8	54
13	$H_4SiMo_{12}O_{40}@SiO_2$	-	60	150	100	100	24
14	$[Eu(PW_{11}O_{39})_2]$/MIL(Al)	-	70	120	500	100	55
15	$[(C_6H_{13})_3PC_{14}H_{29}]_2W_6O_{19}$/G-h-BN	-	30	80	500	99.3	56
16	WO_xNPs/g-BN	-	30	80	500	99.2	57
17	Hexagonal boron nitride nanosheets (h-BNNs)	-	150	180	150	98.8	58
18	Mg_3Al-IL-EuW_{10}	-	60	40	1000	>99	This work
19	Mg_3Al-IL-EuW_{10}	-	70	25	1000	>99	This work

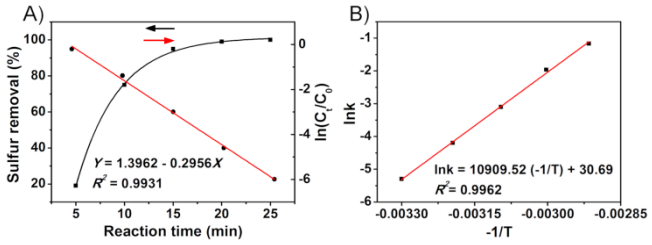

Fig. 6. A) Sulfur removal of DBT (black), ln(C_t/C_0) as a function of reaction time at 70 °C (red); B) Activation energy of desulfurization of DBT. Reaction conditions: H_2O_2/DBT/EuW_{10} = 40:8:1 (t = 25 min, H_2O_2 = 0.08 mL, model oil = 5 mL, S = 1000 ppm).

(min^{-1}) of the pseudo-first-order reaction. The rate constant k of the desulfurization process is determined to be 0.2956 min^{-1} based on the equations (1) and (2) and the activation energy E_a of the catalytic reaction found to be 30.69 kJ/mol according to equation (3) and Fig. S5. As such, the Mg_3Al-IL-EuW_{10} shows high catalytic efficiency for the oxidation of sulfide to sulfone, and the desulfurization process obeys pseudo-first-order reaction.

$$-\mathrm{d}C/\mathrm{d}t = kC \quad (1)$$

$$\ln(C_t/C_o) = -kt \quad (2)$$

$$\ln k = \ln A - \mathrm{Ea}/\mathrm{RT} \quad (3)$$

3.4 Recyclability of the composite material

In an effort to determine the recyclability of the Mg_3Al-IL-EuW_{10}, the catalyst was removed by filtration from the reaction mixture, washed with methanol (3 × 20 mL) and dried at 60 °C overnight. No detectable S element can be observed in the elemental analysis of the recycled catalyst, demonstrating no adsorbed sulfone species. As shown in Fig. 7A, the recycled Mg_3Al-IL-EuW_{10} can be reused for at least 20 times and only then the sulfur removal decreases slightly from 99.9 % to 93 %. XRD patterns, FT-IR, ^{29}Si CP/MAS NMR etc (Fig. 7 and Fig. S6) verify that the catalyst retained its structural integrity and composition during consecutive catalytic and recycling cycles. The observed structural stability of Mg_3Al-IL-EuW_{10} is due to the 2D confinement effect of LDHs and the multiple interactions between the host layers, ILs and guest POMs.

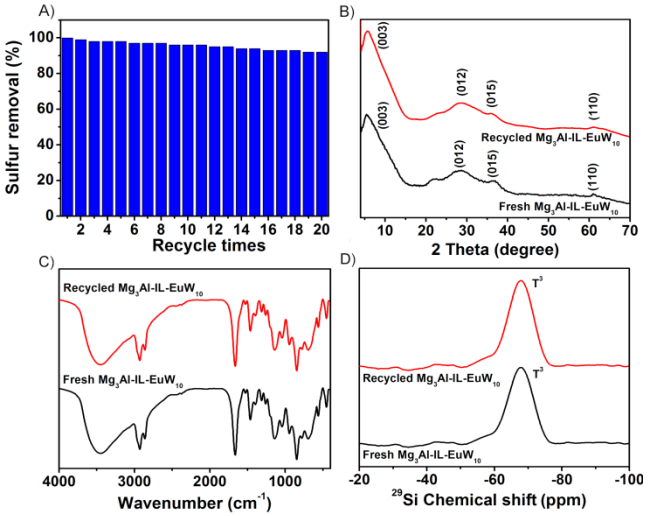

Fig. 7. A) The recycling performance of the catalytic system at 70 °C. Reaction conditions: H_2O_2/DBT/EuW_{10} = 40:8:1 (t = 25 min, H_2O_2 = 0.08 mL, model oil = 5 mL, S = 1000 ppm,); B) XRD patterns, C) FT-IR spectra and D) The ^{29}Si CP/MAS NMR spectra of recycled and fresh Mg_3Al-IL-EuW_{10}.

3.5. Mechanism of reaction

The proposed reaction mechanism for ECODS of DBT is illustrated in Fig. 8. The substrate is extracted from the oil phase to the interface through hydrophobic interactions by the dihydroimidazolium-based ionic liquid covalently linked with LDHs layers. At the same time, EuW_{10} is activated to form the active W-peroxo species in the presence of H_2O_2.[24] Then, the sulfur-containing substrates can access the active centres of the catalyst are oxidized efficiently to the related sulfones.

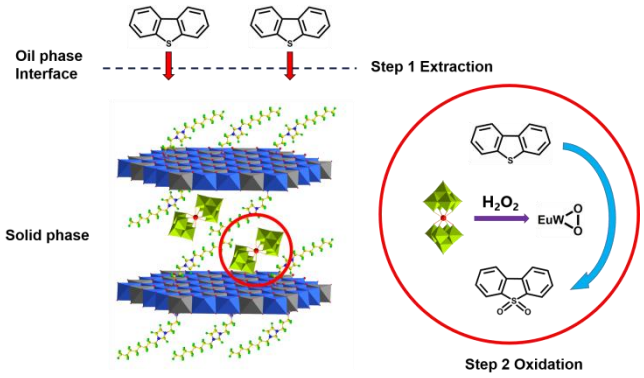

Fig. 8. Proposed mechanism of the desulfurization of oil mixture by Mg_3Al-IL-EuW_{10}.

4. Conclusions

In summary, based on rational design of a heterogeneous catalyst for desulfurization, we have prepared the Mg_3Al-IL-EuW_{10} composite adopting an exfoliation/assembly appeoach. The resultant catalyst shows almost 100 % sulfur removal of DBT, 4,6-DMDBT and BT at 70 °C in 25, 30 and 40 min, respectively, in the presence of H_2O_2. Compared with other ECODS catalytic systems reported so far, the Mg_3Al-IL-EuW_{10} does not need addition, separation and purification of ILs after every catalytic cycle since ILs have been covalently grafted onto the LDHs layers. The excellent structural stability of Mg_3Al-IL-EuW_{10} is retained due to the multiple interactions (extended H-bond network and electrostatic interactions) between the three components (host layers, ILs and POM cluster). Moreover, the heterogeneous catalyst can be separated easily by simple filtration and recycled at least ten times without obvious decrease of its catalytic activity. This work demonstrates for the first time a new design approach for the preparation of polyoxometalate (POM)-based ionic liquid-modified layered double hydroxides (LDHs) for deep desulfurization processes and provides a potentially universal new design strategy for the development of heterogeneous catalysts for various large scale applications.

Acknowledgements

This research was supported by the National Basic Research Program of China (973 program, 2014CB932104), National Science Foundation of China (U1407127, U1507102), Fundamental Research Funds for the Central Universities (YS1406), China Postdoctoral Science Foundation (2014M560878). H.N.M acknowledges the financial support from University of Glasgow.

Notes and references

1 B. Jiang, H. Yang, L. Zhang, R. Zhang, Y. Sun and Y. Huang, *Chem. Eng. J.*, 2016, **283**, 89.
2 V. C. Srivastava, *RSC Adv.*, 2012, **2**, 759.
3 N. Q. Bui, C. Geantet and G. Berhault, *J. Catal.*, 2015, **330**, 374.
4 Y. Wang, C. Lancelot, C. Lamonier, M. Yang, Y. Sun, J. C. Morin and A. Rives, *RSC Adv.*, 2015, **5**, 74150.
5 S. Wang, H. Ge, S. Sun, J. Zhang, F. Liu, X. Wen, X. Yu, L. Wang, Y. Zhang, H. Xu, J. C. Neuefeind, Z. Qin, C. Chen, C. Jin, Y. Li, D. He and Y. Zhao, *J. Am. Chem. Soc.*, 2015, **137**, 4815.
6 L. Haandel, M. Bremmer, P. J. Kooyman, J. A. R. Veen, T. Weber and E. J. M. Hensen, *ACS Catal.*, 2015, **5**, 7276.
7 F. Cui, G. Li, X. Li, M. Lu and M. Li, *Catal. Sci. Technol.*, 2015, **5**, 549.
8 C. Shi, W. Wang, N. Liu, X. Xu, D. Wang, M. Zhang, P. Sun and T. Chen, *Chem. Commun.*, 2015. **51**, 11500.
9 Q. Zhou, S. Fu, M. Zou, Y. He, Y. Wu and T. Wu, *RSC Adv.*, 2015, **5**, 69388.
10 J. Chen, C. Chen, R. Zhang, L. Guo, L. Hua, A. Chen, Y. Xiu, X. Liu and Z. Hou, *RSC Adv.*, 2015, **5**, 25904.
11 W. Dai, G. Li, L. Wang, B. Chen, S. Shang, Y. Lv and S. Gao, *RSC Adv.*, 2014, **4**, 46545.
12 P. S. Kulkarni and C. A. M. Afonso, *Green Chem.*, 2010, **12**, 1139.
13 A. Bosmann, L. Datsevich, A. Jess, A. Lauter, C. Schmitz and P. Wasserscheid, *Chem. Commun.*, 2001, **23**, 2494.
14 W. Zhu, C. Wang, H. Li, P. Wu, S. Xun, W. Jing, Z. Chen, Z. Zhao and H. Li, *Green Chem.*, 2015, **17**, 2464.
15 H. Li, Y. Chang, W. Zhu, W. Jing, M. Zhang, J. Xia, S. Yin and H. Li, *J. Phys. Chem. B*, 2015, **119**, 5995.
16 R. Abro, A. A. Abdeltawab, S. S. Al-Deyab, G. Yu, A. B. Qazi, S. Gao and X. Chen, *RSC Adv.*, 2014, **4**, 35302.
17 H. Gao, M. Luo, J. Xing, Y. Wu, Y. Li, W. Li, Q. Liu and H. Liu, *Ind. Eng. Chem. Res.*, 2008, **47**, 8384.
18 G. Parkinson, *Chem. Eng.*, 2001, **108**, 37.
19 Y. Chen, S. Zhao and Y. F. Song, *Appl. Catal. A: Gen.*, 2013, **466**, 307.
20 X. Zhang, G. Luo, M. Zhu, L. Kang, F. Yu and B. Dai, *RSC Adv.*, 2015, **5**, 76182.
21 S. O. Ribeiro, D. Julião, L. Cunha-Silva, V. F. Domingues, R. Valença, J. C. Ribeiro, B. de Castroa and S. S. Balula, *Fuel*, 2016, **166**, 268.
22 E. Rafiee and F. Mirnezami, *J. Mol. Liq.*, 2014, **199**, 156.
23 S. Xun, W. Zhu, F. Zhu, Y. Chang, D. Zheng, Y. Qin, M. Zhang, W. Jiang and H. Li, *Chem. Eng. J.*, 2015, **280**, 256.
24 Y. Chen and Y.-F. Song, *ChemPlusChem*, 2014, **79**, 304.
25 K. Yamaguchi, C. Yoshida, S. Uchida and N. Mizuno, *J. Am. Chem. Soc.*, 2005, **127**, 530.
26 R. D. Peacock, and T. J. R. Weakley, *J. Chem. Soc. (A)*, 1971, 1836.
27 N. Iyi, Y. Ebina, and T. Sasaki, *J. Mater. Chem.*, 2011, **21**, 8085.
28 Y. Jia, S. Zhao and Y. F. Song, *Appl. Catal. A: Gen.*, 2014, **487**, 172.
29 Y. Jia, Y. Fang, Y. Zhang, H. N. Miras and Y. F. Song, *Chem. Eur. J.,* 2015, **21**, 14862.
30 S. Lis and S. But, *Mater. Sci. Forum*, 1999, **315-317**, 431.

31 C. S. Kan, and J. H. Blackson, *Macromolecules*,1996, **29**, 6853.
32 B. Sels, D. D. Vos, M. Buntinx, F. Pierard, A. K. D. Mesmaeker and P. Jacobs, *Nature*, 1999, **400**, 855.
33 S. Zhao, J. Xu, M. Wei and Y.-F. Song, *Green Chem.*, 2011, **13**, 384.
34 Z. P. Xu and H. C. Zeng, *Chem. Mater.*, 2001, **13**, 4555.
35 M. Sugeta and T. Yamase, *Bull. Chem. Soc. Jpn.*, 1993, **66**, 444.
36 K. S. Sing, D. H. Everett, R. A. W. Haul, L. Moscou, R. A. Pierotti, J. Rouquérol and T. Siemieniewska, *Pure Appl. Chem.*, 1985, **57**, 603.
37 H. Xu, H. Zhao, H. Song, Z. Miao, J. Yang, J. Zhao, N. Liang and L. Chou, *J. Mol. Catal. A: Chem*., 2015, **410**, 235.
38 K. C. Vrancken, L. D. Coster, P. V. D. Voort, P. J. Grobet and E. F. Vansant, *J. Colloid. Interf. Sci.*, 1995, **170**, 71.
39 L. Wei, K. J. T. Livi, W. Xu, M. G. Siebecker, Y. Wang, B. L. Phillips and D. L. Sparks, *Environ. Sci. Technol.,* 2012, **46**, 11670.
40 D. Liang, W. Yue, G. Sun, D. Zheng, K. Ooi and X. Yang, *Langmuir*, 2015, **31**, 12464.
41 C. Yin, G. Zhu and D. Xia, *Fuel Process. Technol.*, 2002, **79**, 135.
42 S. Otsukl, T. Nonaka, N. Takashima, W. Qian, A. Ishihara, T. Imai and T. Kabe, *Energ. Fuel.*, 2000, **14**, 1232.
43 J. L. García-Gutiérrez, G. A. Fuentes, M. E. Hernández-Terán, P. García, F. Murrieta-Guevara and F. Jiménez-Cruz, *Appl. Catal. A: Gen.,* 2008, **334**, 366.
44 L. Qiu, Y. Cheng, C. Yang, G. Zeng, Z. Long, S. Wei, K. Zhao and L. Luo, *RSC Adv.,* 2016, **6**, 17036.
45 M. A. Ramos-Luna and L. Cedeño-Caero, *Ind. Eng. Chem. Res.,* 2011, **50**, 2641.
46 M. A. Cortes-Jácome, M. Morales, C. Angeles-Chavez, L. F. Ramírez-Verduzco, E. López-Salinas and J. A. Toledo-Antonio, *Chem. Mater.,* 2007, **19**, 6605.
47 J. Zhang, A. Wang, Y. Wang, H. Wang and J. Gui, *Chem. Eng. J.,* 2014, **245**, 65.
48 X.-M. Yan, P. Mei, J. Lei, Y. Mi, L. Xiong and L. Guo, *J. Mol. Catal. A: Chem*., 2009, **304**, 52.
49 X.-M. Yan, P. Mei, L. Xiong, L. Gao, Q. Yang and L. Gong, *Catal. Sci. Technol.,* 2013, **3**, 1985.
50 B. Li, W. Ma, J. Liu, C. Han, S. Zuo and X. Li, *Catal. Commun.,* 2013, **13**, 101.
51 L. Tang, G. Luo, M. Zhu, L. Kang and B. Dai, *Ind. Eng. Chem. Res.,* 2013, **19***,* 620.
52 P. Yang, S. Zhou, Y. Du, J. Li and J. Lei, *RSC Adv.,* 2016, **6**, 53860.
53 M. Zhu, G. Luo, L. Kang and B. Dai, *RSC Adv.,* 2014, **4**, 16769.
54 M. Zhang, W. Zhu, H. Li, S. Xun, W. Ding, J. Liu, Z. Zhao and Q. Wang, *Chem. Eng. J.*, 2014, **243**, 386.
55 C. M. Granadeiro, L. S. Nogueira, D. Julião, F. Mirante, D. Ananias, S. S. Balula and L. Cunha-Silva, *Catal. Sci. Technol.*, 2016, **6**, 1515.
56 W. Zhu, B. Dai, P. Wu, Y. Chao, J. Xiong, S. Xun, H. Li and H. Li, *ACS Sus Chem. Eng.*, 2015, **3**, 186.
57 P. Wu, W. Zhu, A. Wei, B. Dai, Y. Chao, C. Li, H. Li and S. Dai, *Chem. Eur. J.*, 2015, **21**, 15421.
58 P. Wu, W. Zhu, Y. Chao, J. Zhang, P. Zhang, H. Zhu, C. Li, Z. Chen, H. Li, and S. Dai, *Chem. Commun.*, 2016, **52**, 144.

Entry for the Table of conntents

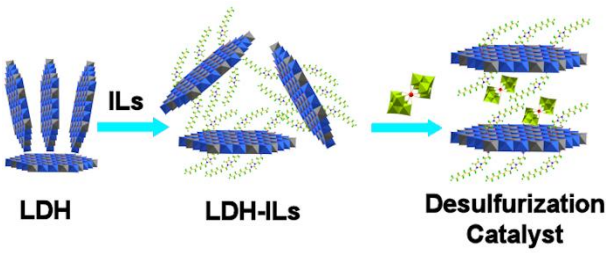

An assembly approach have been employed for the preparation of a multi-component heterogeneous catalyst showing high efficiency in deep desulfurization processes.